TECHNICAL INFORMATION SERIES

R62SD16

APPROXIMATE FLOW CHARACTERISTICS IN THE BASE REGION OF A HYPERSONIC AXI-SYMMETRIC BODY

K.S. WAN

SPACE SCIENCES LABORATORY
GENERAL ELECTRIC
MISSILE AND SPACE DIVISION

SPACE SCIENCES LABORATORY

AEROPHYSICS OPERATION

THE APPROXIMATE FLOW CHARACTERISTICS IN THE BASE REGION OF A HYPERSONIC AXI-SYMMETRIC BODY*

by

K. S. Wan**

*This analysis is based upon work performed under the auspices of the U. S. Air Force Ballistic Systems Division, Contract AF 04(647)-269.

**Research Engineer, Gas Dynamics

R62SD16 - Class I
September, 1962

MISSILE AND SPACE DIVISION

GENERAL ELECTRIC

ABSTRACT

In this report, an approximate method of solution is given to determine the location of the rear stagnation point in the viscous base flow region together with the size of the viscous wake and the flow characteristics there. It is useful as a means of obtaining the initial conditions for the near wake calculations. The results obtained show that one must consider the finite boundary layer at the base in determining the location of the rear stagnation point and the viscous wake width there. In general, the viscous wake at the rear stagnation point consists of a shell of hot gas surrounding a cool core.

CONTENTS

SYMBOLS

x, r	axial and radial coordinates, respectively, non-dimensionalized with respect to $\delta_o = R_B + \delta_B$
ρ	the density non-dimensionalized with respect to ρ_o
u, v	the axial and radial velocity components non-dimensionalized with respect to u_o
p	the static pressure, non-dimensionalized with respect to $1/2\ \rho_o u_o^2$
h	the enthalpy, non-dimensionalized with respect to h_o
p_B	the base pressure
p_∞	the free stream pressure
h_B	the base wall enthalpy, non-dimensionalized with respect to h_o
T_{W_B}	the body wall temperature
R_{eo}	$\frac{\rho_o u_o \delta_o}{\mu_o}$
R_B	the base radius
m	$\frac{u_o^2}{2 h_o}$
s_B	the distance along the body surface from the stagnation point to the corner of the base
P_r	the Prandtl number
δ	the viscous wake width (or radius), non-dimensionalized with respect to δ_o

δ_B the boundary layer thickness at the corner of the base

μ the coefficient of viscosity non-dimensionalized with respect to μ_o

ω $\left(\frac{\partial u}{\partial r}\right)_{r=\delta}$

Ω $\left(\frac{\partial h}{\partial r}\right)_{r=\delta}$

Δ $\int_0^1 \frac{\rho u}{\rho_e u_e} \eta \, d\eta$

Θ $\int_0^1 \frac{\rho u}{\rho_e u_e} \frac{u}{u_e} \eta \, d\eta$

Θ_h $\int_0^1 \frac{\rho u}{\rho_e u_e} \frac{h}{h_e} \eta \, d\eta$

Φ $\int_0^1 \frac{\mu}{\mu_e} \left(\frac{\partial \frac{u}{u_e}}{\partial \eta}\right)^2 \eta \, d\eta$

η $\frac{r}{\delta}$

θ the expansion angle

λ $1 - \eta_d$

η_d as defined in equation (15)

SUBSCRIPTS

e	inviscid condition at the edge of the viscous wake
o	condition at $x = o$
1	condition at the rear stagnation point $x = x_1$

THE APPROXIMATE FLOW CHARACTERISTICS IN THE BASE REGION OF A HYPERSONIC AXI-SYMMETRIC BODY

INTRODUCTION

A theory of base flow for hypersonic axi-symmetric bodies, blunt or slender, has been given in Reference 1. It was developed with the assumption that the gas is in thermo-chemical equilibrium with the Lewis number for the individual chemical species equal to one. The integral method was then used to reduce the governing partial differential equations into ordinary differential equations. The solutions of the resulting equations and the appropriate boundary conditions yielded the detailed flow characteristics in the base region.

In this report, an approximate method is presented by which the location of the rear stagnation point, the size of the viscous wake, and the flow characteristics there can be determined readily. It is developed based on the analysis given in Reference 1 and the following observations.

It is noted first that the integral continuity, momentum and energy equations (Equations (1), (2), and (3) respectively) can be integrated further when the functional form of δ (x) is known. From available shadowgraph pictures on wake flow in the base region, the size of the viscous core is seen to decrease almost conically downstream from the base up to the neck region. Therefore, as a first approximation, one may assume that δ (x) is a linear function of x. Hence, the three equations mentioned previously can be reduced to algebraic equations.

Furthermore, with the occurrence of the recirculating flow in the base region, a rear stagnation point exists which is imbedded in the viscous region and along the axis. Upstream of this point is the recirculating flow region. The flow in the mixing layer above the recirculating flow will go downstream of this point and form the neck and beginning of the near wake. At this point, the velocity component u must also be equal to zero by definition since v is already equal to zero there. This condition reduces the differential equations balancing the momentum and energy along the axis (Equations (5) and (6)) into algebraic

relations. In this manner, a whole set of algebraic equations can be obtained, the solutions of which determine the location of the rear stagnation point and the viscous wake size there, together with the flow characteristics parameters.

The advantages offered by the present method are manifold. The solution of a set of algebraic equations can be more readily obtained than the original differential equations. When the external inviscid flow conditions are uniform (the so-called "free-stream line" case), a table can be generated once and for all to give the solutions in terms of parameters covering a wide range of flight conditions and for different body geometries. Furthermore, the determination of the appropriate boundary for the inviscid flow field, hence the base pressure, requires an iteration procedure between the solutions of the viscous core and the inviscid flow. To accomplish this would be a lengthy and time-consuming process if the theory given in Reference 1 was used repeatedly. This is especially true for a slender body where the base region is expected to be long. Therefore, one can use the method and results given in this report and arrive at a reasonable boundary shape for the inviscid flow field and, hence, the base pressure quickly. Satisfactory results for the details of the viscous flow field in the base region can then be obtained using the complete theory without further iteration.

For a blunt body, the base region is generally short compared with the near and far wake. In this case, the detailed knowledge of the flow characteristics in the base region may not be important with respect to the observables. The present method then gives a good initial flow condition for the near and far wake calculations with the effects of the boundary layer and the subsequent free mixing being accounted for.

For a chemical flow system having a large number of chemical species, the number of equations to be treated will be greatly increased. The understanding of such a complex problem is limited thus far mainly because of the mathematical difficulties presented in solving the large number of differential equations. It is hoped that the present method of approach can be extended to treat such a problem for the base flow. If the governing equations again can be reduced to algebraic

equations in the same manner as in the present case, it is possible that solutions can be obtained in the neck region. The results should serve as a good guide in developing a more complete and detailed theory.

1. THE GOVERNING EQUATIONS

For convenience, the governing equations given in Reference 1 which are pertinent to the present analysis are summarized here.

The continuity, momentum and energy equations after their integrations across the wake are

$$(\rho_e u_e \delta^2 \Delta)' = \rho_e u_e \delta\left(\delta' - \frac{v_e}{u_e}\right) \tag{1}$$

$$(\rho_e u_e^2 \delta^2 \Theta)' = \rho_e u_e^2 \delta\left(\delta' - \frac{v_e}{u_e}\right) - \frac{\delta^2}{4}\frac{dp}{dx} + \frac{\mu_e \delta \omega}{R_{e_o}} \tag{2}$$

$$(\rho_e u_e h_e \delta^2 \Theta_h)' = \rho_e u_e h_e \delta\left(\delta' - \frac{v_e}{u_e}\right) + u_e \delta^2 m \frac{dp}{dx} \Theta_h + \frac{\delta \mu_e}{R_{e_o} P_r} \Omega + \frac{2m \mu_e u_e^2}{R_{e_o}} \Phi \tag{3}$$

where

$$' \equiv \frac{d}{dx}$$

$$\Delta = \int_o^1 \frac{\rho u}{\rho_e u_e} \eta \, d\eta$$

$$\Theta = \int_o^1 \frac{\rho u}{\rho_e u_e} \frac{u}{u_e} \eta \, d\eta$$

$$\Theta_h = \int_o^1 \frac{\rho u}{\rho_e u_e} \frac{h}{h_e} \eta \, d\eta = \int_o^1 \frac{u}{u_e} \eta \, d\eta \text{ assuming that } \frac{\rho h}{\rho_e h_e} = 1$$

$$\omega \equiv \omega(x) = \left(\frac{\partial u}{\partial r}\right)_{r=\delta} = \frac{u_e}{\delta}\left(\frac{\partial \frac{u}{u_e}}{\partial \eta}\right)_{\eta = 1} \tag{4}$$

$$\Omega \equiv \Omega(x) = \left(\frac{\partial h}{\partial r}\right)_{r=\delta} = \frac{h_e}{\delta}\left(\frac{\partial \frac{h}{h_e}}{\partial \eta}\right)_{\eta=1}$$

$$\Phi = \int_0^1 \frac{\mu}{\mu_e}\left(\frac{\partial \frac{u}{u_e}}{\partial \eta}\right)^2 \eta d\eta$$

$$\eta = \frac{r}{\delta}$$

$$R_{e_o} = \frac{\rho_o u_o \delta_o}{\mu_o}$$

$$m = \frac{u_o^2}{2h_o}$$

(4) (cont)

Two more ordinary differential equations are obtained by satisfying the momentum and energy balances along the axis r = 0. They are:

$$\left(\rho u \frac{\partial u}{\partial x}\right)_{\eta=o} = -\frac{1}{2}\frac{dp}{dx} + \frac{2}{\delta^2 R_{e_o}}\left(\mu \frac{\partial^2 u}{\partial \eta^2}\right)_{\eta=o} \quad (5)$$

$$\left(\rho u \frac{\partial h}{\partial x}\right)_{\eta=o} = m(u)_{\eta=0}\frac{dp}{dx} + \frac{2}{\delta^2}\left(\frac{\mu}{P_r R_{e_o}}\frac{\partial^2 h}{\partial \eta^2}\right)_{\eta=o} \quad (6)$$

since v, $\frac{\partial u}{\partial \eta}$ and $\frac{\partial h}{\partial \eta}$ equal to zero at $\eta = o$. The outer boundary conditions

$$\left[\frac{\partial \frac{u}{u_e}}{\partial \eta}\right]_{\eta=1} = \frac{\delta}{u_e}\,\omega(x) \quad (7)$$

$$\left[\frac{\partial \frac{h}{h_e}}{\partial \eta}\right]_{\eta = 1} = \frac{\delta}{h_e}\ \Omega(x) \tag{8}$$

give two additional algebraic equations.

The profiles are assumed to be

$$\frac{\rho u}{\rho_e u_e} = F(x, \eta) + a_1(x)(1 - \eta^2) + a_2(x)(1 - \eta^2)^2 + a_3(x)(1 - \eta^2)^3 \tag{9}$$

$$\frac{h}{h_e} = G(x, \eta) + b_1(x)(1 - \eta^2) + b_2(x)(1 - \eta^2)^2 + b_3(x)(1 - \eta^2)^3 \tag{10}$$

where the a's and the b's are the unknown quantities. They satisfy the boundary conditions that

(1) at $\eta = o$, $v = o$, $\frac{\partial u}{\partial \eta} = o$, and $\frac{\partial h}{\partial \eta} = o$ (11)

(2) at $\eta = 1$, $u = u_e$ $v = v_e$ $h = h_e$ and $\rho = \rho_e$ (12)

(3) at $x = o$ $\rho u = F(o, r)$ (13a)

$$h = G(o, r) \tag{13b}$$

where F (o, r) and G (o, r) are the given and known profiles at the base (i.e., x = o). The initial profiles F (x, η) and G (x, η) have been assumed as

$$\left.\begin{aligned} F(x, \eta) &= o \\ G(x, \eta) &= h_B \end{aligned}\right\} \quad \text{for } o \le \eta < \eta_d \tag{14a}$$

$$\left.\begin{aligned} F(x, \eta) &= f\left(\frac{\eta - \eta_d}{1 - \eta_d}\right) \\ G(x, \eta) &= g\left(\frac{\eta - \eta_d}{1 - \eta_d}\right) \end{aligned}\right\} \text{for } \eta_d < \eta \le 1 \tag{14b}$$

where

$$\eta_d = \frac{\delta_d(x)}{\delta(x)} \quad \text{(See Figure 1)}$$

In here, h_B is the assumed constant nondimensionalized wall enthalpy at the base. The functions f and g have the same functional forms as the distributions of the ρu and h across the boundary layer at the corner of the base of the body, respectively. The function η_d was assumed as

$$\eta_d = \frac{\delta_d(x)}{\delta(x)} \begin{cases} = 1 - \dfrac{\delta_B}{\delta(x)} \sqrt{1 + \sigma^2 \dfrac{\mu_e}{\rho_e u_e} \dfrac{x}{s_B}} & \text{for laminar flow} \quad (15a) \\ = 1 - \dfrac{\delta_B}{\delta(x)} \left(1 + \sigma_\epsilon \dfrac{x}{s_B}\right) & \text{for turbulent flow} \quad (15b) \end{cases}$$

where δ_B is the known boundary layer thickness at the base

s_B is the distance along the body surface from the stagnation point to the corner of the base.

The parameter σ (or σ_ϵ) characterizes the relative growth of a laminar (or turbulent) free mixing layer with respect to that of the laminar (or turbulent) boundary layer (Reference 1).

Equations (1) to (3) and (5) to (8) form the basic system for the seven unknowns δ, a_s and b_s.

2. THE APPROXIMATE METHOD OF SOLUTION

(a) The General Case

It is noted that $\delta(x)$ may be assumed, as a good approximation, to vary linearly with x, or

$$\delta = 1 - \frac{1 - \delta_1}{x_1} x \quad (16)$$

where δ_1 is the unknown nondimensionalized wake radius at the unknown location $x = x_1$ of the rear stagnation point. With this assumed functional form (16) for $\delta(x)$, Equations (1), (2) and (3) can be integrated from $x = 0$ to $x = x_1$ to yield

$$\left[\rho_e u_e \delta^2 \Delta\right]_{x = x_1} - \Delta_{x = 0} = \int_0^{x_1} \rho_e u_e \delta \left(\delta' - \frac{v_e}{u_e}\right) dx \tag{17}$$

$$\left[\rho_e u_e^2 \delta^2 \Theta\right]_{x = x_1} - \Theta_{x = 0} = \int_0^{x_1} \left[\rho_e u_e^2 \delta \left(\delta' - \frac{v_e}{u_e}\right) - \frac{dp}{dx} \frac{\delta^2}{4} + \frac{\mu_e \delta}{R_{e_o}} \omega\right] dx \tag{18}$$

$$\mathcal{E}_{h_{x = x_1}} = \mathcal{E}_{h_{x = 0}} e^{-\int_0^{x_1} \Gamma_1(x)\, dx} + e^{-\int_0^{x_1} \Gamma_1(x)\, dx} \times \int_0^{x_1} \Gamma_2(x)\, e^{\int \Gamma_1(x)\, dx}\, dx \tag{19}$$

where

$$\left.\begin{aligned} \Gamma_1(x) &= \frac{\left(\rho_e u_e h_e \delta^2\right)' - u_e \delta^2 m \frac{dp}{dx}}{\rho_e u_e h_e \delta^2} \\ \Gamma_2(x) &= \frac{\rho_e u_e h_e \delta \left(\delta' - \frac{v_e}{u_e}\right) + \frac{\delta \mu_e}{P_r R_{e_o}} \Omega + \frac{2m \mu_e u_e^2}{R_{e_o}} \Phi}{\rho_e u_e h_e \delta^2} \end{aligned}\right\} \tag{20}$$

The right-hand sides of Equations (17), (18) and (19) are all integrable as the functions ρ_e, u_e, v_e, h_e, μ_e, $\frac{dp}{dx}$, λ and Ω are all given functions and $\delta(x)$ is assumed as in (16). One exception is the function Φ which is the dissipation existed in the flow. In the base region, the contribution to the dissipation due to the recirculating flow is expected to be small. Hence, as an approximation, one may consider only the dissipation from the boundary layer flow and the subsequent free mixing in the calculation of the function Φ. In other words, Φ will be calculated by considering only the terms $F(x, \eta)$ and $G(x, \eta)$ in the assumed profiles. Therefore, Φ is also a known function of x.

Equations (17), (18) and (19) are three algebraic equations relating the known inviscid flow conditions to the unknowns δ_1, x_1, and other unknowns in the assumed profiles. Additional algebraic equations are now obtained by considering the conditions at the rear stagnation point.

By definition, at the rear stagnation point $x = x_1$ and $r = o$, the velocity component us must be equal to zero since $v = o$ at $r = o$ in general. Therefore, from (9) one has

$$a_{11} + a_{21} + a_{31} = 0 \tag{21}$$

and from (5) and (6)

$$\left(- \frac{1}{2} \frac{dp}{dx} \right)_1 + \frac{2}{R_{e_o} \delta_1^2} \left(\mu_e u_e \frac{\partial^2 \frac{u}{u_e}}{\partial \eta^2} \right)_{\substack{\eta = o \\ x = x_1}} = 0$$

$$\left[\frac{\partial^2 \frac{h}{h_e}}{\partial \eta^2} \right]_{\substack{\eta = o \\ x = x_1}} = 0$$

The last two equations can be reduced to, from the assumed profiles (9) and (10),

$$\left(-\frac{1}{2}\frac{dp}{dx}\right)_1 + \frac{2(\mu_e u_e)_1}{R_{e_o}\delta_1^2}\left[(g_o + b_{11} + b_{21} + b_{31})^2 \times (-2a_{11} - 4a_{21} - 6a_{31})\right] = 0 \tag{22}$$

$$2b_{11} + 4b_{21} + 6b_{31} = 0 \tag{23}$$

where a_{11}, a_{21}, a_{31}, b_{11}, b_{21}, and b_{31} are their respective values at $x = x_1$. Furthermore, a_{11} and b_{11} should satisfy the following relations through (7) and (8):

$$a_{11} = \frac{1}{2}\left(F_{e_1}' - \frac{\delta_1}{u_1}\omega_1 + \frac{\delta_1}{h_1}\Omega_1\right) \tag{24}$$

$$b_{11} = \frac{1}{2}\left(G_{e_1}' - \frac{\delta_1}{h_1}\Omega_1\right) \tag{25}$$

where

$$F_{e_1}' = \left(\frac{\partial F}{\partial \eta}\right)_{\substack{\eta = 1 \\ x = x_1}}$$

$$G_{e_1}' = \left(\frac{\partial G}{\partial \eta}\right)_{\substack{\eta = 1 \\ x = x_1}}$$

Equations (17) to (19) and (21) to (25) are the eight algebraic equations to be solved simultaneously for the eight unknowns, x_1, δ_1, a_s and the b_s. In the general case, they can be reduced into three algebraic equations for x_1, δ_1, and a_{21}. When the external velocity and enthalpy gradients are negligible, i.e., F_e', G_e', ω and Ω are approximately equal to zero, a_{11} and b_{11} are equal to zero according to equations (24) and (25). The remaining equations can then be reduced to two equations for x_1 and δ_1 in such a case.

(b) The "Free-Stream Line" Case

For the particular case when the external inviscid flow conditions are uniform, the so-called "free-stream line" case, the set of equations given in the previous section offers a convenient way for solutions. In this case, Equations (17) to (19) and (21) to (23) can be rewritten and reduced into

$$\delta_1^2 \Delta_1 = \Delta_o - \left(\frac{1 - \delta_1}{x_1} + v_o \right) \left(1 - \frac{1 - \delta_1}{2} \right) x_1 \tag{26}$$

$$\delta_1^2 \Theta_1 = \Theta_o - \left(\frac{1 - \delta_1}{x_1} + v_o \right) \left(1 - \frac{1 - \delta_1}{2} \right) x_1 \tag{27}$$

$$\delta_1^2 \Theta_{h_1} = \Theta_{h_o} - \left(\frac{1 - \delta_1}{x_1} + v_o \right) \left(1 - \frac{1 - \delta_1}{2} \right) x_1 + \int_o^{x_1} \frac{2m}{R_{e_o}} \Phi \, dx \tag{28}$$

$$a_{21} + a_{31} = 0 \tag{29}$$

$$2a_{21} + 3a_{31} = 0 \tag{30}$$

$$2b_{21} + 3b_{31} = 0 \tag{31}$$

From (29) and (30), one has $a_{21} = a_{31} = 0$ and from (31) $b_{31} = (-2/3)b_{21}$. Therefore, there are only three unknowns, δ, x_1, and b_{21} left to be solved from Equations (26) to (28). It can be shown that, in general, Θ_1 and Θ_{h_1} are linear functions of b_{21}. Therefore, b_{21} can be eliminated simply by combining Equations (27) and (28). The resulting equation together with Equation (26) determines δ_1 and x_1. A convenient method of solution for these equations can be devised such that tables can be generated once and for all to give solutions in

terms of parameters covering a wide range of flight conditions and for different body geometries. This will be explained in detail in the following section.

3. NUMERICAL PROCEDURES

For illustrative purpose, let us consider the "free stream-line" case and assume that

$$\left.\begin{aligned} F(x, \eta) &= 0 \\ G(x, \eta) &= h_B \end{aligned}\right\} \quad \text{for } 0 \le \eta < \eta_d \tag{32a}$$

$$\left.\begin{aligned} F(x, \eta) &= \frac{\eta - \eta_d}{1 - \eta_d} \\ G(x, \eta) &= h_B + (1 - h_B)\left(\frac{\eta - \eta_d}{1 - \eta_d}\right) \end{aligned}\right\} \text{for } \eta_d < \eta \le 1 \tag{32b}$$

In this case, it can be shown that

$$\left.\begin{aligned} \Delta_o &= \frac{1}{2}\lambda_o - \frac{1}{6}\lambda_o^2 \\ \Delta_1 &= \frac{1}{2}\lambda_1 - \frac{1}{6}\lambda_1^2 \\ \Theta_o &= \left(\frac{h_B}{3} + \frac{1 - h_B}{4}\right)\lambda_o - \left(\frac{h_B}{12} + \frac{1 - h_B}{20}\right)\lambda_o^2 \\ \Theta_1 &= \left(\frac{h_B}{3} + \frac{1 - h_B}{4}\right)\lambda_1 - \left(\frac{h_B}{12} + \frac{1 - h_B}{20}\right)\lambda_1^2 \\ &\quad + \left(\frac{2}{15}\lambda_1^3 - \frac{2}{9}\lambda_1^4 + \frac{8}{63}\lambda_1^5\right) b_{21} = \Theta_{11} + \Theta_{21} b_{21} \\ \Theta_{h_o} &= \left(\frac{h_B}{2} + \frac{1 - h_B}{3}\right)\lambda_o - \left(\frac{h_B}{6} + \frac{1 - h_B}{12}\right)\lambda_o^2 \end{aligned}\right\} \tag{33}$$

$$\left.\begin{aligned}
\Theta_{h_1} &= \left(\frac{h_B}{2} + \frac{1 - h_B}{3}\right)\lambda_1 - \left(\frac{h_B}{6} + \frac{1 - h_B}{12}\right)\lambda_1^2 \\
&\quad + \left(\frac{1}{3}\lambda_1^3 - \frac{2}{3}\lambda_1^4 + \frac{4}{9}\lambda_1^5\right) b_{21} \\
&= \Theta_{h_{11}} + \Theta_{h_{21}} b_{21}
\end{aligned}\right\} \quad (33)\ (\text{cont})$$

where

$$\lambda_o = \delta_B$$

$$\lambda_1 = 1 - \eta_{d_1} = \begin{cases} \dfrac{\delta_B}{\delta_1}\sqrt{1 + \sigma^2 \dfrac{x_1}{s_B}} & \text{for laminar flow} \\ \dfrac{\delta_B}{\delta_1}\left(1 + \sigma_\epsilon \dfrac{x_1}{s_B}\right) & \text{for turbulent flow} \end{cases} \quad (34)$$

Also

$$\int_o^{x_1} \frac{2m}{R_{e_o}} \Phi \, dx = \frac{2mx_1}{R_{e_o}} \, \omega \, (h_B, \lambda_o, \lambda_1, \delta_1)$$

Therefore, Equations (27) and (28) can be combined to eliminate b_{21}. This gives, after simplification,

$$\Theta_{h_{21}} (\Theta_o - \Theta_{11} \delta_1^2) - \Theta_{21} (\Theta_{h_o} - \Theta_{h_{11}} \delta_1^2)$$

$$= (\Theta_{h_{21}} - \Theta_{21}) \left(\frac{1 - \delta_1}{x_1} + v_o\right)\left(1 \frac{1 - \delta_1}{2}\right) x_1 + \frac{2m\,\varphi}{R_{e_o}} \Theta_{21} x_1 \quad (35)$$

In principle, then, δ_1, and x_1 can be obtained by solving Equations (26) and (35). However, λ_1 is a function of both the unknowns x_1 and δ_1 for a given

condition [Equation (34)]. Therefore, to obtain the solution of the simultaneous equations for δ_1 and x_1 directly will require a somewhat lengthy and laborious procedure. But a convenient way for solutions can be obtained in the following manner.

Let us rewrite (26) to give

$$\left(\frac{1-\delta_1}{x_1} + v_o\right)\left(1 - \frac{1-\delta_1}{2}\right) x_1 = \Delta_o - \delta_1^2 \Delta_1 \tag{36}$$

and

$$x_1 = \frac{2\left(\Delta_o - \delta_1^2 \Delta_1 - \frac{1-\delta_1^2}{2}\right)}{v_o(1+\delta_1)}$$

Putting these into Equation (35), one has

$$(1+\delta_1)\left\{\delta_1^2\left[\Theta h_{21}(\Delta_1 - \Theta_{11}) - \Theta_{21}(\Delta_1 - \Theta h_{11})\right]\right.$$

$$\left. + \left[\Theta h_{21}(\Theta_o - \Delta_o) - \Theta_{21}(\Theta h_o - \Delta_o)\right]\right. \tag{37}$$

$$= \frac{4m\varphi}{v_o R e_o}\left[\delta_1^2\left(\Delta_1 + \frac{1}{2}\right) - \left(\Delta_o + \frac{1}{2}\right)\right]$$

This equation gives δ_1 as a function of h_B, m, Re_o, v_o, λ_o, and λ_1 where λ_1 is a function of $\delta_B(=\lambda_o)$, σ(or σ_ϵ), s_B, x_1 and δ_1. For a given body geometry at given flight conditions, m, Re_o, $\delta_B(=\lambda_o)$, s_B are known quantities and for an assumed expansion angle around the corner of the base (or assumed base pressure), h_B, v_o and σ (or σ_ϵ) can be determined. To solve for δ_1 and x_1 one may assume a value of λ_1 which varies from λ_o to one and solve for δ_1, from (37) for a given set of values of h_B, m, Re_o, v_o, λ_o, σ (or σ_ϵ) and s_B. x_1 is then determined from (36). For this set of values of x_1 and δ_1, λ_1 can be calculated from (34) for the same given values of δ_B, σ and s_B. This calculated value of λ_1 should check with the assumed λ_1 value when δ_1 and x_1 are the correct solutions to both Equations (35) and (26).

However, this trial and error procedure is not really necessary. Instead, one may solve for δ_1 from (37) and then x_1 from (36) assuming a series of values of λ_1 from λ_o to one for a given set of values h_B, m, R_{e_o}, v_o, λ_o and s_B. σ and σ_ϵ are then calculated from [see (34)].

$$\sigma = \sqrt{\frac{s_B}{x_1}\left[\left(\frac{\lambda_1 \delta_1}{\delta_B}\right)^2 - 1\right]} \tag{38a}$$

$$\sigma_\epsilon = \frac{s_B}{x_1}\left(\frac{\lambda_1 \delta_1}{\delta_B} - 1\right) \tag{38b}$$

In this manner, tables can be generated beforehand to give the values of δ_1, x_1, σ and σ_ϵ as functions of λ_1 for a given set of values of h_B, v_o, λ_o, s_B, m and R_{e_o}. For a particular case of interest, one merely has to go to these tables and find out the values of δ_1 and x_1 for a particular set of values of h_B, v_o, λ_o, s_B, m, R_{e_o} and σ (or σ_ϵ). The corresponding value of λ_1 which gives the ratio of the thickness of the mixing layer to the viscous wake width at the rear stagnation point can also be obtained.

To summarize, the numerical procedure consists of: (1) construction of tables (or graphs) giving values of σ, σ_ϵ, δ_1, x_1, and b_{21} (from Equations (38a), (38b), (37), (36), and (27) respectively) as functions of λ_1 for sets of assigned values of s_B, $\lambda_o (= \delta_B)$, m, R_{e_o}, v_o, and h_B. (2) For a particular case of interest, s_B is known from the given body geometry. $\lambda_o (= \delta_B)$, m, and R_{e_o} can be obtained from the known or calculated inviscid shock layer flow and the boundary layer flow for a given flight condition. (3) Assume a base pressure value hence the value of the expansion angle θ and determine the values of $v_o = -\tan\theta$, h_B and σ (or σ_ϵ). (4) The solutions for δ_1, x_1, and b_{21} are then obtained from the tables for this set of values of s_B, λ_o, m, R_{e_o}, v_o, h_B and σ (or σ_ϵ).

It should be remarked that λ_1 varies between λ_o and one only since $\eta_{d_1} = \delta_{d_1}/\delta_1$ can not be negative [see Equation (34)]. Also the value of σ (or σ_ϵ) is greater than one in actual case because the growth of a free mixing layer is larger than that of a boundary layer under the same condition.

4. RESULTS AND DISCUSSIONS

Results given in this section are for the "free-stream line" case with $F(x, \eta)$ and $G(x, \eta)$ given in (32a) and (32b).

Tables I(A) and (B) give part of the results obtained in the manner described in step (1) of the preceding section. In these calculations, the term on the right hand side of (37) has been found to be small and hence neglected. These two tables are obtained for $s_B = 4$, $v_o = -0.06993.$, $h_B = 2$ and $1/2$ with $\lambda_o = 0.1$ for table I(A) and $\lambda_o = 0.001$ for table I(B). The range of σ values covered is approximately from 3.2 to 1.

Figures 2a and 2b are plots of the results given in Tables IA and IB, respectively. They show that δ_1 decreases and x_1 increases with σ except that δ_1 increases slightly beyond $\sigma \cong 2.8$ in the case of $\lambda_o = 0.1$. Figure 2a shows further that δ_1 increases and x_1 decreases with h_B in the case of $\lambda_o = 0.1$ but they are practically unchanged with h_B for $\lambda_o = 0.001$. However, it should be remembered that v_o, h_B and σ are not independent of each other but rather they are related through the base pressure (or the expansion angle) assumed. Therefore, one should not draw any definite conclusion from results such as in Table IA (or Figure 2A) in regard to the variations of δ_1, and x_1 with respect to σ or h_B independently for a particular given case since neither σ nor h_B is a single independent variable parameter. This will be further explained later in this section.

However, one can draw a conclusion as to the effect of the finite boundary layer at the base from these results. Figure 3 is a plot of δ_1 and x_1 vs σ for $\delta_B = 0.1$ and 0.001 with the same values of s_B, v_o and h_B. Since for a given body geometry, flight conditions and an assumed expansion angle, the values of s_B, v_o, h_B, σ and δ_B (say 0.1) are known and fixed, therefore, this figure compares the results of δ_1 and x_1 from the "actual" case ($\delta_B = 0.1$ case) with the case where δ_B is assumed negligible ($\delta_B = 0.001$ case). It is seen that if δ_B is neglected, δ_1 is much smaller and x_1 much larger than the actual case. The discrepancy increases with increasing σ and varies from 15% to 50% for δ_1 and 30% to 50% for x_1. This can be explained as follows. For an initial boundary layer of small

but finite thickness at the base, the volume of gas $\left[V_o = 1 - (1 - \delta_B)^2\right]$ contained in the boundary layer there is not negligibly small. In the axi-symmetric case, the total volume of this gas surrounding the base converges to the axis to form the core at the rear stagnation point. The radius of this core must be sufficiently large so that this finite volume of gas will be contained there. When the initial boundary layer at the base is neglected, under the same conditions, the core size will be naturally much smaller since there will be very little volume of gas to be contained in the core in this case. At the same time, x_1 will be larger for the expansion angle (or base pressure). With a larger value of σ, more volume of gas will be drawn from outside into the mixing layer and hence, the difference in δ_1 and x_1 will become larger between the two cases. These results, therefore, emphasize the importance of the inclusion of the finite boundary layer in treating the base flow for an axi-symmetric body.

Table II gives results for the specific case of a 20^o sphere cone at M_∞ = 19.52 and altitude = 150,000 feet. They are obtained according to the procedure described in the preceding section. In these calculations, two constant body wall temperature values T_{W_B} (2 and 1/2 corresponding to hot and cool wall) have been assumed and the δ_B values were estimated. In each case, five expansion angles and their respective base pressure values were assumed and the corresponding sets of values of v_o, h_B and σ were determined. The solution for δ_1, x_1, b_{21} and the value of λ_1 were then obtained from the table.

These results show that δ_1 decreases and x_1 increases with increasing T_{W_B} or h_B for the same base pressure or with increasing base pressure for the same T_{W_B} or h_B. However, it would be clearer and more meaningful if one uses the parameters x_1 and θ_1 for comparison instead of x_1 and δ_1 where θ_1 denotes the angular position of the edge of the viscous wake with respect to the free stream (see Table II and Figures 4 and 5). These show that θ_1 decreases and x_1 increases with increasing base pressure for the same T_{W_B} or h_B. Since a smaller θ_1 and larger x_1 will give a larger base region, therefore, the larger the assumed base pressure, the larger is the base region. This is expected physically since a higher base pressure can sustain the mixing process longer and a

bigger volume of gas. Furthermore, θ_1 is practically unchanged but x_1 increases with h_B for a given base pressure. This is again because a hot base wall can sustain a longer mixing process. Furthermore, for a hotter base wall but with the same base pressure, the resulting mixing layer at the rear stagnation point is also thicker as it is evident from the larger value of λ_1 and smaller value of δ_{d_1}. This has the same trend as in the case of the boundary layer. However, it is noted that the base pressure and the base wall enthalpy are not two independent parameters. For a given known base wall enthalpy, there is only one corresponding base pressure. This will be a subject for future investigation.

The other interesting results are those of b_{21} and δ_{d_1}. The value of b_{21} is practically zero for all the cases considered. This means that the radial enthalpy distribution at the rear stagnation point in the viscous wake is the same as that at the base but in different scale (see Figure 5). It is further noted that δ_{d_1} is generally nonzero at x_1. In the case of a cool base, this means that a cool core exists there with a shell of hot gas surrounding it. This shell of hot gas is formed mainly by the gas from the boundary layer. For a hot base, the solution shows that the core is hot. However, in the actual case the temperature and enthalpy at the wall of the base probably will vary rather than be uniform as assumed here and decrease from the value at the corner to some lower value at the center. If this is the case, then even for an originally hot body wall, that part of the base near the axis is cool. Therefore, at the rear stagnation point, the core will still be cool but the shell surrounding it will be hot and comparatively thicker than in the case of a cool wall. These phenomena are probably associated with the growth of the mixing layer. Over the extent of the base region, up to the rear stagnation point, there would not be sufficient time or distance for the mixing layer to grow to its fullest before its lower boundary reaches the axis. The heat content is being contained within the mixing layer without too much heat exchange between the mixing layer and the recirculating flow. Therefore, the enthalpy level between the axis and the lower boundary of the mixing layer would be the same as that of the base wall with the enthalpy distribution in the mixing layer remaining the same as in the initial boundary layer. However, future experimental measurements and flight tests for the base region will shed additional light on this problem.

It should be noted that the location of the rear stagnation point does not necessarily coincide with the location of neck which is the narrowest region of the wake. However, the results obtained for the rear stagnation point are necessary for the investigation of the flow in the near wake region.

5. CONCLUSIONS

It can be concluded from the results in the present investigation that one must consider the finite boundary layer at the base in treating the base flow. By neglecting the boundary layer one will overestimate x_1 and underestimate δ_1 by a large percent.

For an uniformly cool base, it was found that a cool core exists at the rear stagnation point with a shell of hot gas surrounding it. This shell of hot gas is formed mainly by the gas from the boundary layer. However, a hot core could be formed there if the base were uniformly hotter than the free stream. The latter case may not be realistic since the base wall temperature will probably decrease from the corner of the base to the axis. Therefore, it is reasonable to say that, in general, a shell of hot gas surrounding a cool core exists at the rear stagnation point.

REFERENCE

1. Wan, K. S. "On a Theory of Base Flow for Hypersonic, Axi-Symmetric Bodies" GE-MSD TIS R62SD15 (In Publication).

ACKNOWLEDGEMENT

The author wishes to thank the staff members of the Gas Dynamics, Aerophysics Operation of the Space Sciences Laboratory, for many helpful discussions during the course of this work, in particular M. E. Long and Dr. K. T. Yen. He would like also to express his appreciations to Mrs. M. Cooke who wrote the program for the numerical calculations and Mrs. M. Oberst who helped in preparing the manuscript.

TABLE I

(A) $\lambda_o = \delta_B = 0.1$, $S_B = 4$

$v_o = -\text{Tan}\,\theta = -0.06993$

(a) $h_B = 2$

σ	σ_ϵ	δ_1	x_1	b_{21}	λ_1
3.1694	1.78	0.4629	8.1324	-0.0848	1
2.8137	1.545	0.4584	8.0949	-0.0767	0.9
2.5080	1.34	0.4603	7.9881	-0.0625	0.8
2.2381	1.17	0.4688	7.8029	-0.0451	0.7
1.9926	1.01	0.4849	7.5215	-0.0286	0.6
1.7621	0.872	0.5107	7.1108	-0.0161	0.5
1.5385	0.738	0.5505	6.5050	-0.0079	0.4
1.3132	0.604	0.6144	5.5606	-0.0032	0.3
1.0741	0.468	0.7288	3.8988	-0.0009	0.2

(b) $h_B = 1/2$

σ	σ_ϵ	δ_1	x_1	b_{21}	λ_1
2.8542	1.55	0.4266	8.4464	-0.0164	1
2.5906	1.375	0.4304	8.3458	-0.0160	0.9
2.3493	1.222	0.4384	8.1906	-0.0141	0.8
2.1246	1.085	0.4516	7.9683	-0.0107	0.7
1.9113	0.956	0.4712	7.6579	-0.0070	0.6
1.7045	0.83	0.4999	7.2230	-0.0039	0.5
1.4990	0.707	0.5422	6.5948	-0.0019	0.4
1.2877	0.587	0.6085	5.6274	-0.0007	0.3
1.0594	0.457	0.7255	3.9390	-0.0002	0.2

TABLE I (Continued)

(B) $\lambda_o = \delta_B = 0.001$, $S_B = 4$

$v_o = -\text{Tan}\,\theta = -0.06993$

(a) $h_B = 2$

σ	σ_ϵ	δ_1	x_1	b_{21}	λ_1
3.6284	1.78	0.1599	12.1182	0	0.04
3.1660	1.54	0.1841	11.7690		0.03
2.6217	1.255	0.2248	11.1814		0.02
1.9170	0.884	0.3170	9.8511		0.01
1.7377	0.788	0.3542	9.3143		0.008
1.5340	0.68	0.4088	8.5271		0.006
1.4192	0.62	0.4477	7.9661		0.005
1.2919	0.555	0.5004	7.2059		0.004
1.1469	0.483	0.5777	6.0916		0.003
0.9739	0.39	0.7073	4.2218	0	0.002

(b) $h_B = 1/2$

σ	σ_ϵ	δ_1	x_1	b_{21}	λ_1
3.6221	1.78	0.1596	12.1218	0	0.04
3.1617	1.54	0.1838	11.7720		0.03
2.6193	1.255	0.2246	11.1839		0.02
1.9161	0.884	0.3169	9.8528		0.01
1.7370	0.788	0.3541	9.3157		0.008
1.5336	0.68	0.4087	8.5283		0.006
1.4188	0.62	0.4476	7.9671		0.005
1.2916	0.555	0.5004	7.2067		0.004
1.1467	0.483	0.5776	6.0922		0.003
0.9738	0.39	0.7073	4.2222	0	0.002

TABLE II

$M_\infty = 19.52$, $H = 150{,}000$ ft, Equilibrium Air, 20° sphere cone, $S_B = 2.92$

T_{W_B}	$\lambda_o = \delta_B$	θ	p_B/p_∞	v_o	h_B	σ	δ_1	x_1	b_{21}	λ_1	$\delta_{d_1} = (1-\lambda_1)\delta_1$	$\tan\theta_1 = \frac{1-\delta_1}{x_1}$
2	0.0668	$12^\circ 54'$	11.766	-0.22903	2.24	3.48	0.40912	2.6144	-0.0379	0.562	0.17919	0.22601
		$17^\circ 36'$	8.83	-0.31722	2.25	3.53	0.424	1.925	-0.0221	0.40	0.216	0.29922
		$22^\circ 24'$	6.54	-0.41217	2.3	3.62	0.448	1.375	-0.015	0.43	0.2555	0.40145
		$35^\circ 12'$	2.767	-0.70064	2.52	3.92	0.5363	0.66665	-0.00627	0.265	0.3942	0.69556
		$48^\circ 30'$	1	-1.1303	2.752	4.28	0.6116	0.345	-0.0035	0.1451	0.5229	1.1258
1/2	0.0437	$12^\circ 54'$	11.766	-0.22903	0.56	2.45	0.4536	2.38973	-0.00032	0.2344	0.3473	0.22865
		$17^\circ 36'$	8.83	-0.31722	0.568	2.48	0.512	1.6	-0.0001	0.188	0.415	0.305
		$22^\circ 24'$	6.54	-0.41217	0.581	2.54	0.572	1.04	0	0.15	0.486	0.41154
		$35^\circ 12'$	2.767	-0.70064	0.63	2.77	0.7073	0.4179	0	0.0911	0.6519	0.70041
		$48^\circ 30'$	1	-1.1303	0.688	3.01	0.8469	0.13565	0	0.062	0.7944	1.12864

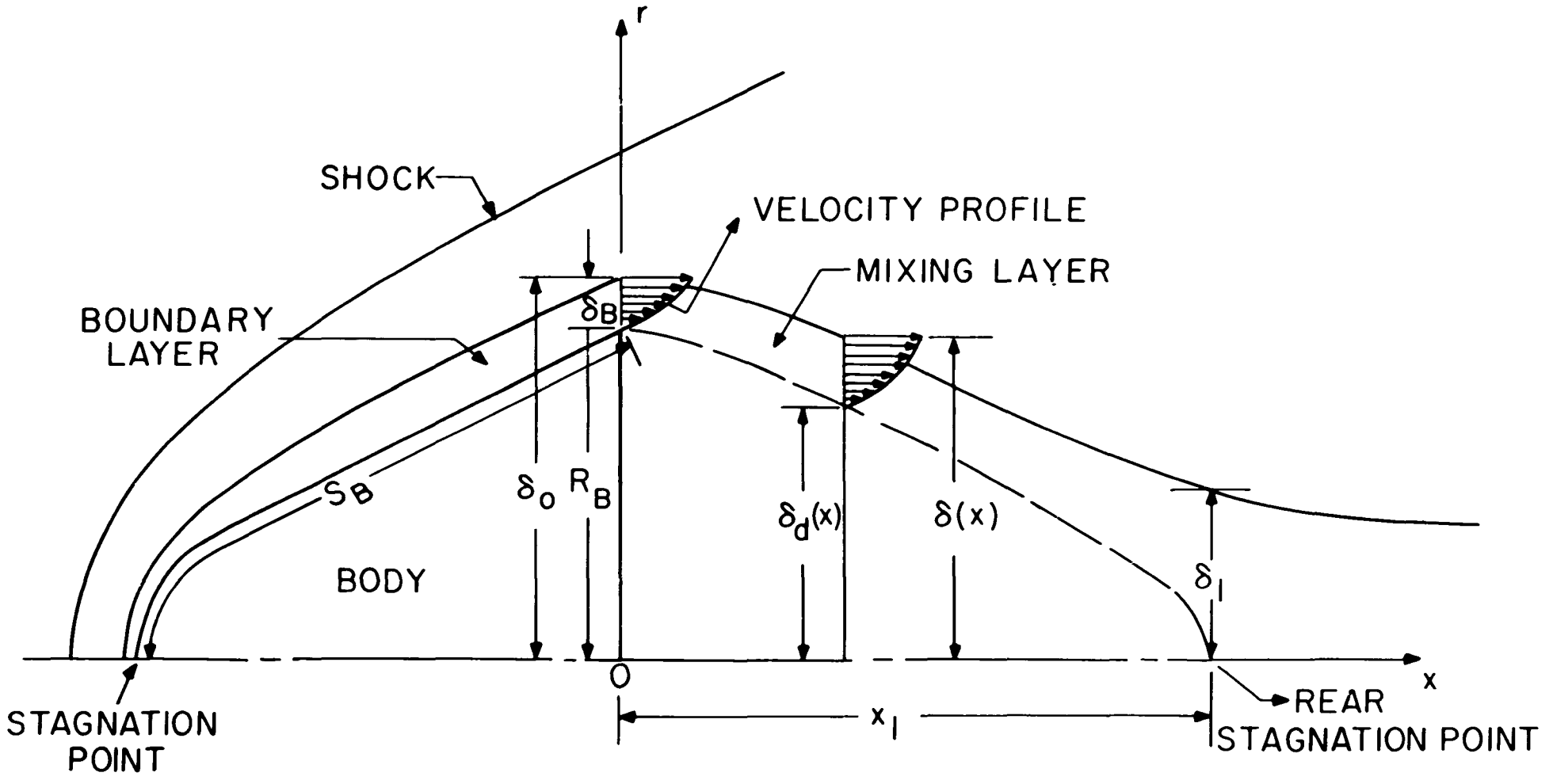

FIGURE I: FLOW IN THE BASE REGION

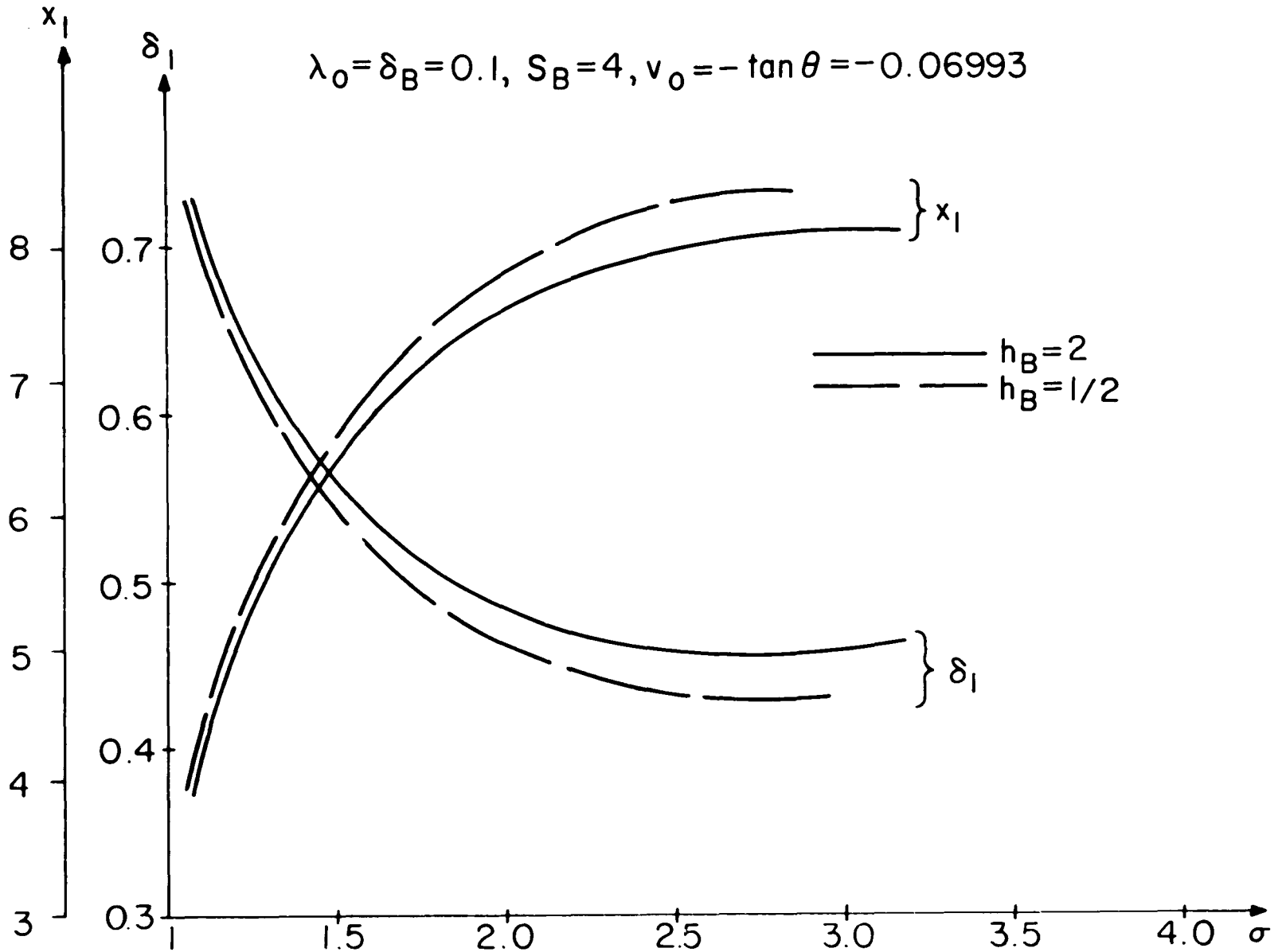

FIGURE 2a: VARIATIONS OF δ_1 & x_1 WITH σ ($\delta_B=0.1$)

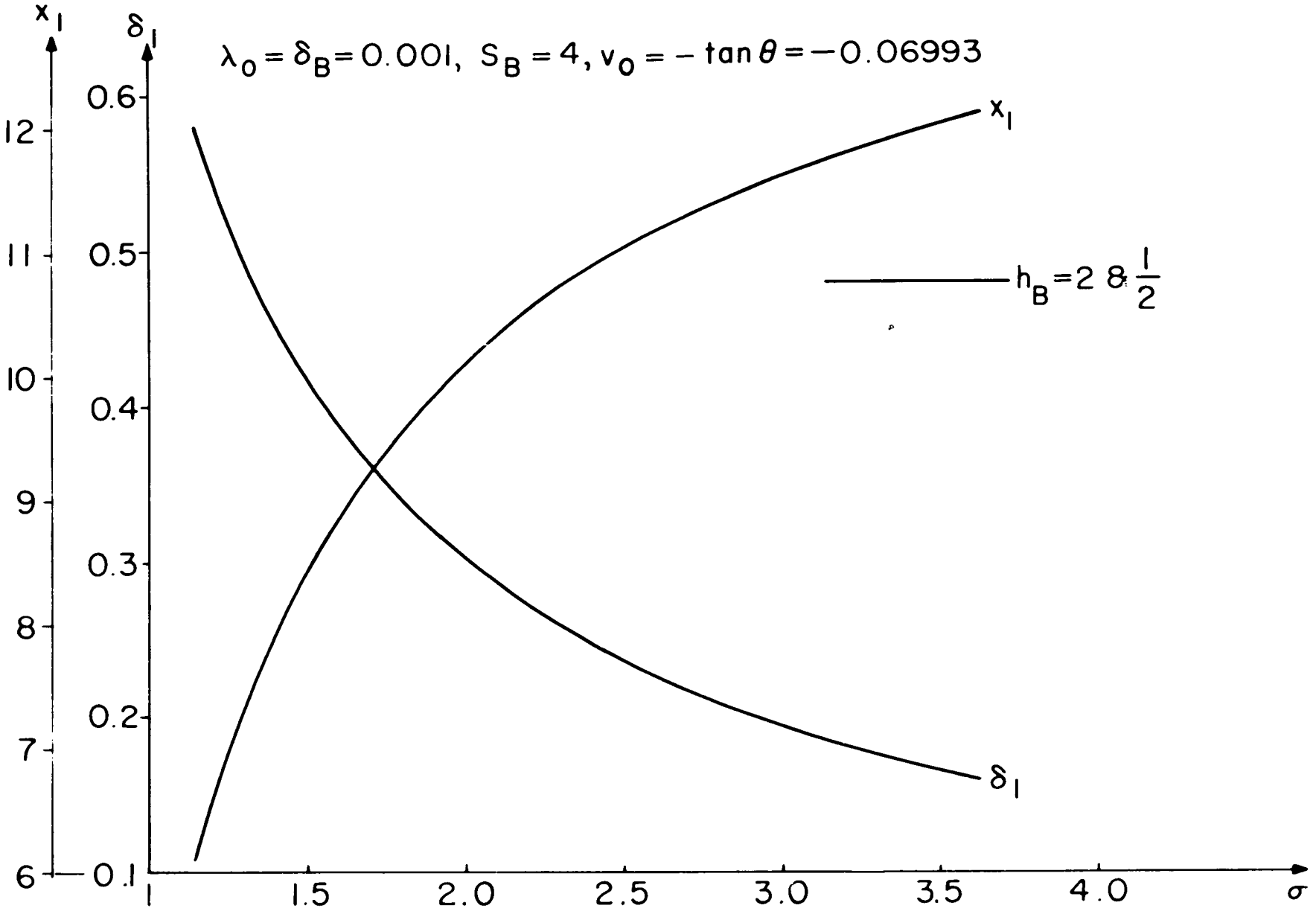

FIGURE 2b: VARIATION OF δ_1 & x_1 WITH σ ($\delta_B = 0.001$)

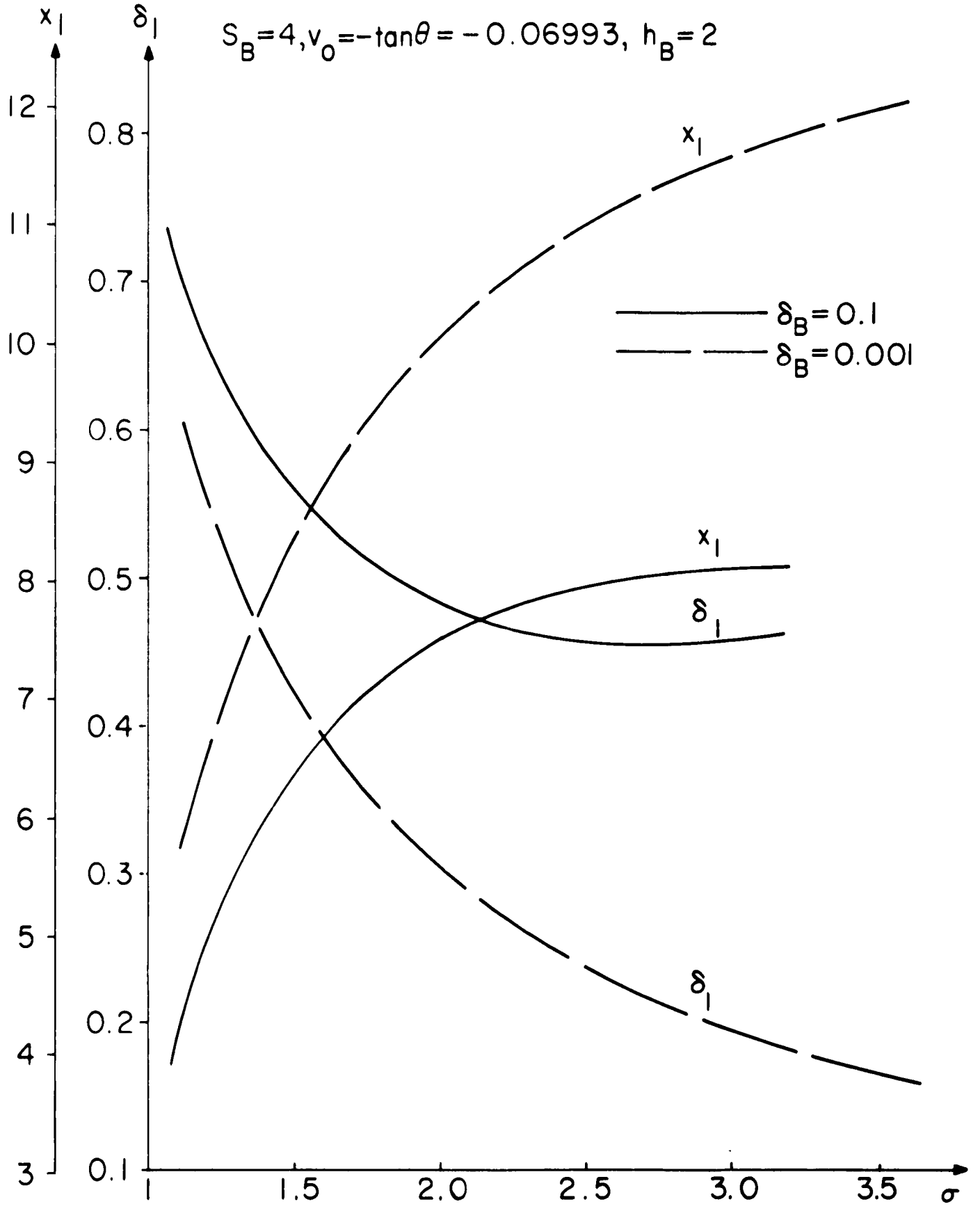

FIGURE 3: EFFECT OF FINITE BOUNDARY LAYER ON δ_1 & x_1

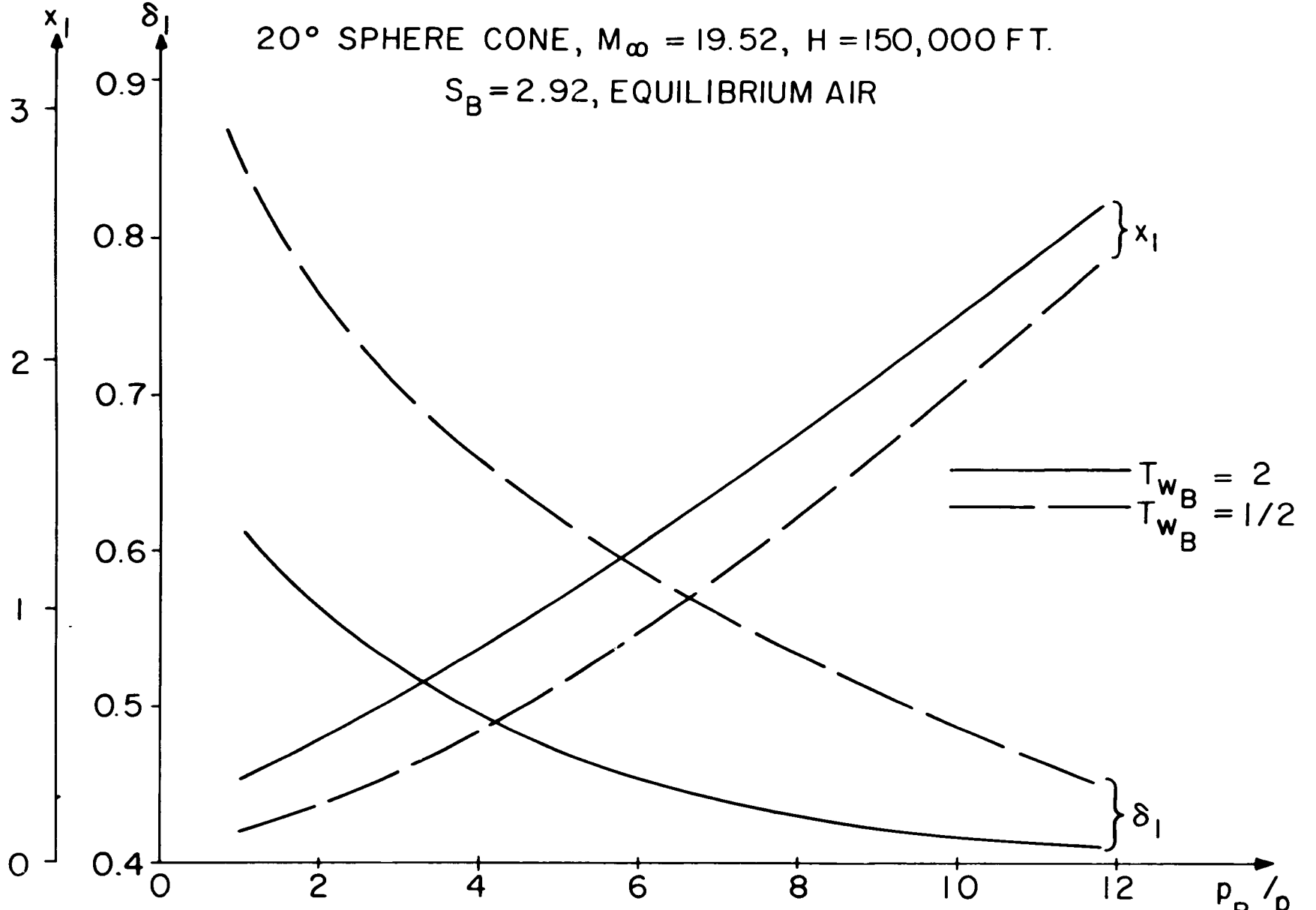

FIGURE 4: VARIATIONS OF δ_1 & x_1 WITH BASE PRESSURE

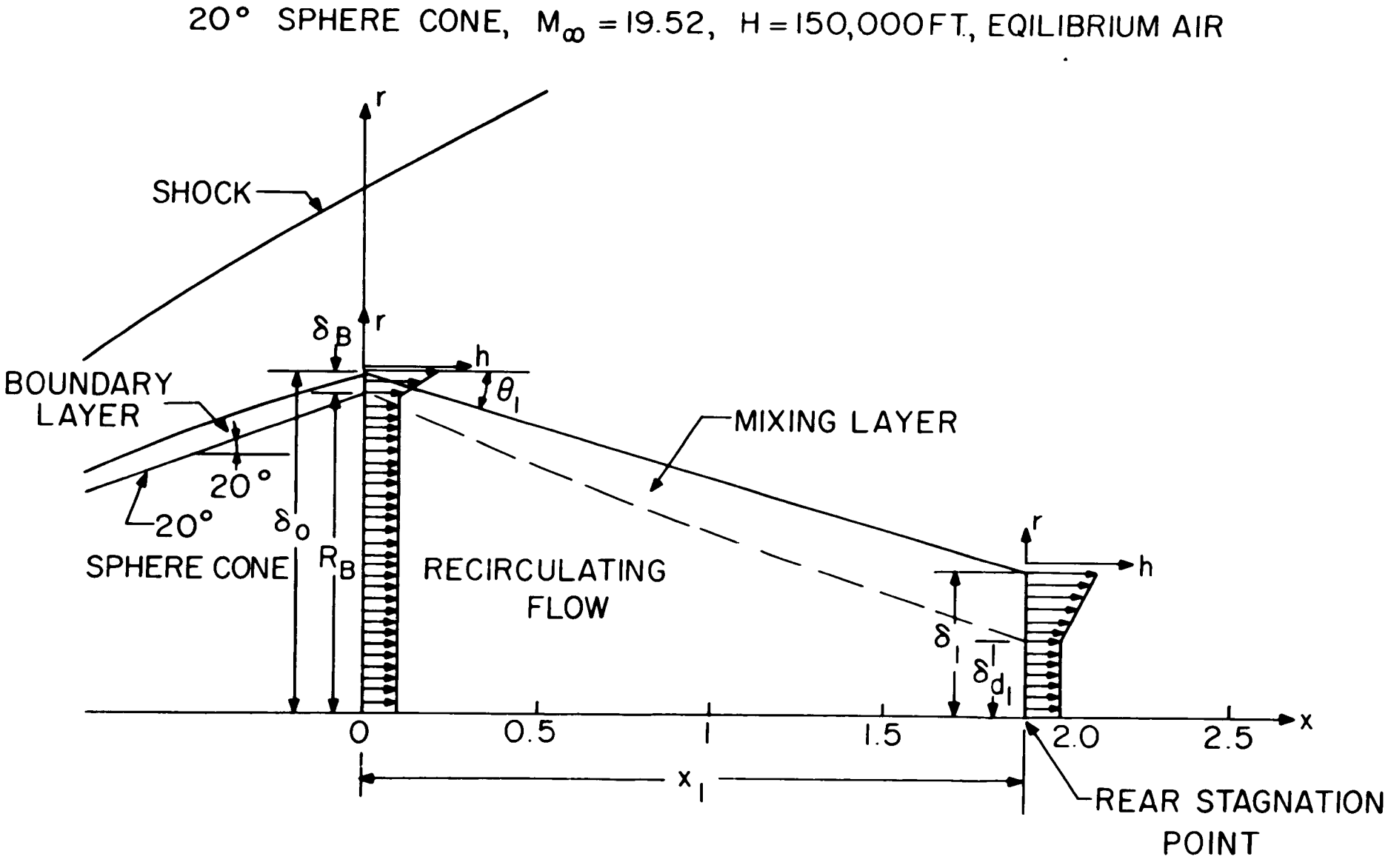

FIGURE 5: ENTHALPY DISTRIBUTIONS IN THE BASE REGION

GENERAL ELECTRIC

SPACE SCIENCES LABORATORY
MISSILE AND SPACE DIVISION

TECHNICAL INFORMATION SERIES

AUTHOR	SUBJECT CLASSIFICATION	NO.
K.S. Wan	Re-entry Physics	R62SD16
		DATE: Sept. 1962
TITLE: Approximate Flow Characteristics In The Base Region Of A Hypersonic Axi-symmetric Body		G. E. CLASS: I
		GOV. CLASS: None
REPRODUCIBLE COPY FILED AT MSD LIBRARY, DOCUMENTS LIBRARY UNIT, VALLEY FORGE SPACE TECHNOLOGY CENTER, KING OF PRUSSIA, PA.		NO. PAGES: 34

SUMMARY

In this report, an approximate method of solution is given to determine the location of the rear stagnation point in the viscous base flow region together with the size of the viscous wake and the flow characteristics there. It is useful as a means of obtaining the initial conditions for the near wake calculations. The results obtained show that one must consider the finite boundary layer at the base in determining the location of the rear stagnation point and the viscous wake width there. In general, the viscous wake at the rear stagnation point consists of a shell of hot gas surrounding a cool core.

By cutting out this rectangle and folding on the center line, the above information can be fitted into a standard card file.

AUTHOR K. S. Wan

COUNTERSIGNED F. T. C. Lew Joseph Fabri